Int. J. Solids Structures Vol. 16, pp. 625–644

0020-7683/80/0701-0625/$02.00/0

QUASI-STATIC BENDING OF A CYLINDRICAL ELASTIC BAR PARTIALLY EMBEDDED IN A SATURATED ELASTIC HALF-SPACE

V. APIRATHVORAKIJ and P. KARASUDHI
Division of Structural Engineering and Construction, Asian Institute of Technology, P.O. Box 2754, Bangkok, Thailand

(*Received* 14 *June* 1979; *in revised form* 13 *November* 1979)

Abstract—This paper presents the quasi-static behavior of a circular cylindrical elastic bar which is partially embedded in a saturated elastic half-space. The bar is subjected to a lateral force and a moment at a top end. The material of the half-space is governed by Biot's consolidation theory. The problem is decomposed into two systems; namely, an extended half-space and a fictitious bar with a Young's modulus equal to the difference between the Young's moduli of the real bar and the half-space. The governing equation, which is formulated under the approximation that the slope of the fictitious bar is equal to the corresponding average over a circular area in the extended half-space, is found to be a Fredholm integral equation of the second kind, and solved by an appropriate numerical method for initial and final solutions.

NOTATION

- a radius of circular cylindrical bar and nondimensionalizing constant
- A cross sectional area of bar, nondimensionally equal to π
- B domain of the extended half-space, Fig. 4(a)
- B_* fictitious bar, Fig. 4(b)
- c coefficient of consolidation of the half-space defined by eqn (2d)
- D region of bar in domain B, Fig. 4(a)
- E Young's modulus of the half-space
- E_p, E_* Young's moduli of real and fictitious bars, respectively
- G shear modulus of the half-space $= E/2(1+\nu)$
- I moment of inertia of bar cross section, nondimensionally equal to $\pi/4$
- J_m Bessel function of the first kind and m th order
- L embedded length of bar
- M, M_* moments of real and fictitious bars, respectively
- M_o applied moment at $x_3 = 0$
- p_f excess pore pressure
- $q(z)$ linear intensity of the force in region D
- Q, Q_* shear of real and fictitious bars, respectively
- Q_o applied lateral force at $x_3 = 0$
- r radial coordinate
- t time nondimensionalized by a^2/c
- $u(\bar{x})$ displacement in x_1-direction at a point $\bar{x}$ in domain B
- $u_*(z)$ displacement in x_1-direction at a point $x_3 = z$ of both fictitious and real bars
- x_1, x_2, x_3 cartesian coordinates
- $\bar{x}$ cartesian position vector, having x_1, x_2 and x_3 as orthogonal components
- z x_3
- θ angular coordinate
- ν Poisson's ratio of the half-space
- $\pi_z, \bar{\pi}_z$ open and closed cross sections of region D at $x_3 = z$ in Fig. 4(a) respectively
- σ_{ij} cartesian stress components
- $\Psi_*(z, z')$ slope function of fictitious bar defined by eqn (21)
- Ψ_o rigid body rotation of the fictitious bar

1. INTRODUCTION

The diffusion of load from an embedded elastic bar into an elastic half-space has been a subject of interest and an object of numerous investigations, chiefly because of their relevance to the analysis and design of such structures as anchor-bar systems, pile-supported foundations, off-shore structures, etc. Muki and Sternberg[1] made a pilot study on the diffusion of an axial load from an infinite cylindrical bar fully immersed in an infinite elastic medium, and later[2] investigated the case of an axial load in a cylindrical bar that is partially embedded in an elastic half-space. Niumpradit[3] extended the work of Muki and Sternberg[2] to the quasi-statics of a porous elastic half-space completely saturated with water.

All studies mentioned above are confined to the case of axisymmetrical load-transfer problems. The case of asymmetrical problems, such as the problem of an elastic bar partially

embedded in an elastic half-space and subjected to a lateral force and a moment at the top end, have many practical applications. Early analyses of this type for pile foundation problems completely ignored the soil resistance and the ends of the piles were treated as either pinned or fixed, thus resulted in extremely conservative predictions. Later, the theory of subgrade reaction in which the embedding soil is replaced by an elastic spring of the Winkler's type was employed. Such treatment is still unsatisfactory, as the continuity of the soil mass is not taken into account properly, and frequently leads to incorrect results. Spillers and Stoll[4] presented a method for analysis of piles of any flexibilities by considering the soil mass to be an elastic continuum and felt that a continuum approach would be more rational than a Winkler's type analysis. Poulos[5] made a further study with an analysis which is similar in principle to that employed by Spillers and Stoll[4], but a more refined assumption regarding pile action. A comparative study between the elastic and subgrade reaction solutions shows that the subgrade reaction theory is inaccurate but on the safe side, especially in case of very flexibile piles.

However, the assumption that the medium is an ideal elastic solid is not satisfactory for cases where the medium contains a fluid, such as in case of soil systems or in some biomechanic applications. For such cases, it is more realistic to assume that the medium is a porous elastic solid filled with fluid and behaves according to the theory developed some years ago by Biot[6–8]. Biot's equations satisfy not only the requirements for the deformation of the solid matrix but also the Darcy's law for the fluid flowing in the medium.

The main objective of this paper is to investigate rigorously the quasi-static bending of an elastic circular cylindrical bar, partially embedded in a porous elastic half-space. The embedding medium is assumed to be isotropic homogeneous and completely saturated. The problem is formulated by using an approximative scheme similar to that used by Muki and Sternberg[2] for the case of an elastostatic load-transfer to a half-space from an axially loaded bar. The governing equation of the problem is found to be a Fredholm integral equation of the second kind and can be solved by an appropriate numerical method. Numerical results of initial and final solutions are obtained and presented. The final solution can be shown to be identical to that of the ideal elastostatic problem, but the present approach should be considered as more refined than all existing elastostatic treatments.

2. QUASI-STATICS OF COMPLETELY SATURATED MEDIUM

According to the consolidation theory of Biot[6–8] for a completely saturated and isotropic medium, the quasi-static governing equations can be written in terms of displacements and the excess pore pressure, with a cylindrical coordinate system (r, θ, z) as the reference, as follows

$$\nabla^2 u_r + (2\eta - 1)\frac{\partial e}{\partial r} - \frac{1}{r}\left[\frac{2}{r}\frac{\partial u_\theta}{\partial \theta} + \frac{u_r}{r}\right] + \frac{\partial p_f}{G\partial r} = 0 \tag{1a}$$

$$\nabla^2 u_\theta + (2\eta - 1)\frac{\partial e}{r\partial \theta} - \frac{1}{r}\left[\frac{u_\theta}{r} - \frac{2}{r}\frac{\partial u_r}{\partial \theta}\right] + \frac{\partial p_f}{Gr\partial \theta} = 0 \tag{1b}$$

$$\nabla^2 u_z + (2\eta - 1)\frac{\partial e}{\partial z} + \frac{\partial p_f}{G\partial z} = 0 \tag{1c}$$

$$\nabla^2 e = \frac{\partial e}{c\partial t} \tag{1d}$$

where u_r, u_θ and u_z are displacements of the solid matrix in r, θ and z directions, respectively; p_f is the excess pore pressure (positive if tension), t is the time variable and

$$\nabla^2 = \frac{\partial^2}{\partial r^2} + \frac{1}{r}\frac{\partial}{\partial r} + \frac{1}{r^2}\frac{\partial^2}{\partial \theta^2} + \frac{\partial^2}{\partial z^2} \tag{2a}$$

$$e = \frac{\partial u_r}{\partial r} + \frac{u_r}{r} + \frac{1}{r}\frac{\partial u_\theta}{\partial \theta} + \frac{\partial u_z}{\partial z} \tag{2b}$$

$$\eta = \frac{1-\nu}{1-2\nu}, \qquad c = \frac{2G\eta k}{\rho}. \tag{2c, d}$$

In addition, ∇^2 is the Laplace operator, e is the dilatation, ν and G are ratio and shear modulus of the medium, c is the coefficient of consolidation, ρ is the unit weight of the water and k is the coefficient of permeability of the medium.

For reasons of convenience; it is appropriate to nondimensionalize the problem by defining a, which denotes the radius of the embedded bar, as a unit of length; and a^2/c as a unit of time. All notations previously defined can still be used as dimensionless quantities, however c must be taken as unity from now on. It should also be noted that the final ($t = \infty$) solution is identical to the ideal elastostatic solution since the excess pore pressure p_f tends to zero there.

General solution to eqns (1) can be obtained by means of the auxiliary functions as suggested by Schiffman and Fungaroli[9], together with the technique of Fourier expansions for θ variable and Hankel transform for r variable as proposed by Muki[10] for elastostatics. Accordingly, the displacements and excess pore pressure may be written in the following forms

$$u_r(r, \theta, z, t) = \sum_{m=0}^{\infty} u_{rm}(r, z, t) \cos m\theta \tag{3a}$$

$$u_\theta(r, \theta, z, t) = \sum_{m=0}^{\infty} u_{\theta m}(r, z, t) \sin m\theta \tag{3b}$$

$$u_z(r, \theta, z, t) = \sum_{m=0}^{\infty} u_{zm}(r, z, t) \cos m\theta \tag{3c}$$

$$\frac{1}{2G} p_f(r, \theta, z, t) = \sum_{m=0}^{\infty} p_{fm}(r, z, t) \cos m\theta \tag{3d}$$

where, for each harmonic m,

$$\begin{aligned} u_{rm} + u_{\theta m} = \frac{1}{2\pi i} \int_0^{\infty} \int_{\alpha - i\infty}^{\alpha + i\infty} \xi^2 J_{m+1}(\xi r)\, e^{pt} [&- \xi A_m e^{-z\xi} - \gamma B_m e^{-z\gamma} \\ &+ \xi C_m e^{z\xi} + \gamma D_m e^{z\gamma} - z E_m e^{-z\xi} - z F_m e^{z\xi} \\ &+ 2G_m e^{-z\xi} + 2H_m e^{z\xi}]\, dp\, d\xi \end{aligned} \tag{4a}$$

$$\begin{aligned} u_{rm} - u_{\theta m} = \frac{1}{2\pi i} \int_0^{\infty} \int_{\alpha - i\infty}^{\alpha + i\infty} \xi^2 J_{m-1}(\xi r)\, e^{pt} [&\xi A_m e^{-z\xi} + \gamma B_m e^{-z\gamma} \\ &- \xi C_m e^{z\xi} - \gamma D_m e^{z\gamma} + z E_m e^{-z\xi} + z F_m e^{z\xi} \\ &+ 2G_m e^{-z\xi} + 2H_m e^{z\xi}]\, dp\, d\xi \end{aligned} \tag{4b}$$

$$\begin{aligned} u_{zm} = \frac{1}{2\pi i} \int_0^{\infty} \int_{\alpha - i\infty}^{\alpha + i\infty} \xi J_m(\xi r)\, e^{pt} [&- \xi^2 A_m e^{-z\xi} - \gamma^2 B_m e^{-z\gamma} \\ &- \xi^2 C_m e^{z\xi} - \gamma^2 D_m e^{z\gamma} - (1 + z\xi) E_m e^{-z\xi} \\ &- (1 - z\xi) F_m e^{z\xi}]\, dp\, d\xi \end{aligned} \tag{4c}$$

$$\begin{aligned} p_{fm} = \frac{1}{2\pi i} \int_0^{\infty} \int_{\alpha - i\infty}^{\alpha + i\infty} \xi J_m(\xi r) e^{pt} [&- \eta\gamma(\gamma^2 - \xi^2) B_m e^{-z\gamma} \\ &+ \eta\gamma(\gamma^2 - \xi^2) D_m e^{z\gamma} + \xi E_m e^{-z\xi} - \xi F_m e^{z\xi}]\, dp\, d\xi \end{aligned} \tag{4d}$$

where p is the parameter of Laplace transforms for time variable t, i is the imaginary constant, α is a real number greater than the highest real part of singularities of the Laplace transform involved, J_m is the Bessel function of the first kind of order m, A_m to H_m are constants of integration to be determined from appropriate boundary and continuity conditions, and

$$\gamma = (\xi^2 + p)^{1/2}. \tag{5}$$

Similarly, the stress components may be written in the following forms

$$\frac{1}{2G}\sigma_{rr}(r,\theta,z,t)=\sum_{m=0}^{\infty}\sigma_{rrm}(r,z,t)\cos m\theta \tag{6a}$$

$$\frac{1}{2G}\sigma_{\theta\theta}(r,\theta,z,t)=\sum_{m=0}^{\infty}\sigma_{\theta\theta m}(r,z,t)\cos m\theta \tag{6b}$$

$$\frac{1}{2G}\sigma_{zz}(r,\theta,z,t)=\sum_{m=0}^{\infty}\sigma_{zzm}(r,z,t)\cos m\theta \tag{6c}$$

$$\frac{1}{2G}\sigma_{r\theta}(r,\theta,z,t)=\sum_{m=0}^{\infty}\sigma_{r\theta m}(r,z,t)\sin m\theta \tag{6d}$$

$$\frac{1}{2G}\sigma_{\theta z}(r,\theta,z,t)=\sum_{m=0}^{\infty}\sigma_{\theta m}(r,z,t)\sin m\theta \tag{6e}$$

$$\frac{1}{2G}\sigma_{zr}(r,\theta,z,t)=\sum_{m=0}^{\infty}\sigma_{zrm}(r,z,t)\cos m\theta \tag{6f}$$

where, for each harmonic m,

$$\begin{aligned}\sigma_{rrm}+\frac{1}{r}u_{rm}+\frac{m}{r}u_{\theta m}=\frac{1}{2\pi i}\int_0^{\infty}\int_{\alpha-i\infty}^{\alpha+i\infty}\xi J_m(\xi r)e^{pt}[&-\xi^3A_m\,e^{-z\xi}-\gamma^3B_m\,e^{-z\gamma}\\&+\xi^3C_m\,e^{z\xi}+\gamma^3D_m\,e^{z\gamma}+\xi(1-z\xi)E_m\,e^{-z\xi}\\&-\xi(1+z\xi)F_m\,e^{z\xi}]dp\,d\xi\end{aligned} \tag{7a}$$

$$\begin{aligned}\sigma_{rrm}+\sigma_{\theta\theta m}=\frac{1}{2\pi i}\int_0^{\infty}\int_{\alpha-i\infty}^{\alpha+i\infty}\xi J_m(\xi r)e^{pt}[&-\xi^3A_m\,e^{-z\xi}-\gamma(2\gamma^2-\xi^2)B_m\,e^{-z\gamma}\\&+\xi^3C_m\,e^{z\xi}+\gamma(2\gamma^2-\xi^2)D_m\,e^{z\gamma}+\xi(2-z\xi)E_m\,e^{-z\xi}\\&-\xi(2+z\xi)F_m\,e^{z\xi}]dp\,d\xi\end{aligned} \tag{7b}$$

$$\begin{aligned}\sigma_{zzm}=\frac{1}{2\pi i}\int_0^{\infty}\int_{\alpha-i\infty}^{\alpha+i\infty}\xi^2J_m(\xi r)e^{pt}[&\xi^2A_m\,e^{-z\xi}+\gamma\xi B_m\,e^{-z\gamma}\\&-\xi^2C_m\,e^{z\xi}-\gamma\xi B_m\,e^{z\gamma}+(1+z\xi)E_m\,e^{-z\xi}\\&-(1-z\xi)F_m\,e^{z\xi}]dp\,d\xi\end{aligned} \tag{7c}$$

$$\begin{aligned}\sigma_{\theta zm}+\sigma_{zrm}=\frac{1}{2\pi i}\int_0^{\infty}\int_{\alpha-i\infty}^{\alpha+i\infty}\xi^2J_{m+1}(\xi r)e^{pt}[&\xi^2A_m\,e^{-z\xi}+\gamma^2B_m\,e^{-z\gamma}\\&+\xi^2C_m\,e^{z\xi}+\gamma^2D_m\,e^{z\gamma}+z\xi E_m\,e^{-z\xi}-z\xi F_m\,e^{z\xi}\\&-\xi G_m\,e^{-z\xi}+\xi H_m\,e^{z\xi}]dp\,d\xi\end{aligned} \tag{7d}$$

$$\begin{aligned}\sigma_{\theta zm}-\sigma_{zrm}=\frac{1}{2\pi i}\int_0^{\infty}\int_{\alpha-i\infty}^{\alpha+i\infty}\xi^2J_{m-1}(\xi r)e^{pt}[&\xi^2A_m\,e^{-z\xi}+\gamma^2B_m\,e^{-z\gamma}\\&+\xi^2C_m\,e^{z\xi}+\gamma^2D_m\,e^{z\gamma}+z\xi E_m\,e^{-z\xi}-z\xi F_m\,e^{z\xi}\\&+\xi G_m\,e^{-z\xi}-\xi H_m\,e^{z\xi}]dp\,d\xi\end{aligned} \tag{7e}$$

$$\sigma_{r\theta m}+\frac{m}{r}u_{rm}+\frac{1}{r}u_{\theta m}=\frac{1}{2\pi i}\int_0^{\infty}\int_{\alpha-i\infty}^{\alpha+i\infty}\xi^2J_m(\xi r)\,e^{pt}[\xi G_m\,e^{-z\xi}+\xi H_m\,e^{z\xi}]dp\,d\xi. \tag{7f}$$

The final step to obtain the solution is to invert the integral transforms involved. For the Laplace transform, it is quite difficult and laborious if standard exact or asymptotic methods are used to obtain its inverse. Several approximate inversion methods have been developed specifically for various quasi-static problems. Among these methods, the approximation technique proposed by Schapery[11] has been found to be very accurate for viscoelasticity and also

for the case of a saturated elastic half-space loaded by a normal patch load on the surface of the half-space[3]. This Schapery's scheme says that a time function $f(t)$ can be determined from its Laplace transform $\bar{f}(p)$ according to the following simple formula

$$f(t) \simeq [p\bar{f}(p)]_{p=0.5/t}. \tag{8}$$

Another good property of this formula is that it guarantees exact initial ($t = 0^+$) and final ($t = \infty$) values. Only these two extreme solutions will be considered in this paper.

It would be shown in a later section that the inverse Hankel transforms involved, in obtaining the initial and final solutions, are integrals of the Lipschitz–Hankel type involving products of Bessel functions. These integrals can be determined by various formulae developed by Eason, Noble and Sneddon[12].

3. FUNDAMENTAL SOLUTIONS

At this step, it is appropriate to first derive the solutions for the cases of a uniform shearing force and a linearly varying normal force acting over a circular area of radius a in the interior and on the surface of the half-space, as shown in Figs. 1 and 2, respectively. These solutions would serve as the fundamental solutions necessary for solving the main problem.

Uniform shearing force in the interior of the half-space

For the case of a uniform shearing force of unit intensity acting over a circular area of a radius a at a depth z' as shown in Fig. 1, the problem is symmetric with respect to $\theta = 0$ axis, and the general solution denoted by eqns (3) and (6) is simply given by the harmonic terms with $m = 1$ only. The load is applied as a time step function.

The problem can be solved by taking the half-space as divided into upper and lower domains by an imaginary horizontal plane at the depth z' where the force is and using superscripts 1 and 2 to denote these respective domains. In view of eqns (4) and (7); constants C_1^2, D_1^2, F_1^2 and H_1^2 of domain 2 must vanish to guarantee the boundedness of the solution as z approaches infinity. Thus there are twelve constants to be determined from the boundary and continuity conditions; i.e. A_1^1, B_1^1, C_1^1, D_1^1, E_1^1, F_1^1, G_1^1, H_1^1 of domain 1, and A_1^2, B_1^2, E_1^2, G_1^2 of domain 2.

The boundary conditions for the free and permeable surface at $z = 0$, $t > 0$ and $0 \le r < \infty$ are

$$\sigma_{zz}^1(r, \theta, 0, t) = 0, \qquad \sigma_{z\theta}^1(r, \theta, 0, t) = 0 \tag{9a, b}$$

$$\sigma_{zr}^1(r, \theta, 0, t) = 0, \qquad p_f^1(r, \theta, 0, t) = 0. \tag{9c, d}$$

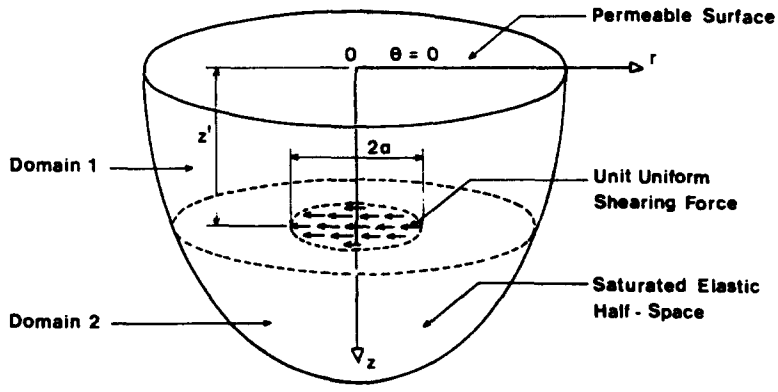

Fig. 1. Uniform shearing force in the interior of the half-space.

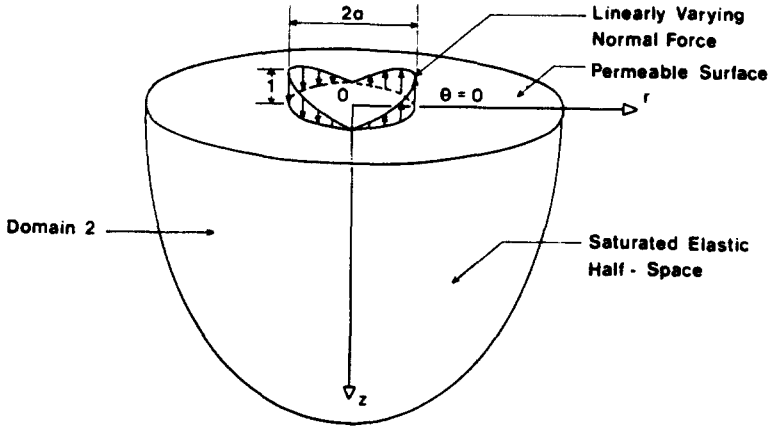

Fig. 2. Linearly varying force on the surface of the half-space.

The continuity conditions at $z = z'$, $t > 0$ and $0 \le r < \infty$ are

$$u_r^1(r, \theta, z', t) = u_r^2(r, \theta, z', t) \tag{10a}$$

$$u_\theta^1(r, \theta, z', t) = u_\theta^2(r, \theta, z', t) \tag{10b}$$

$$u_z^1(r, \theta, z', t) = u_z^2(r, \theta, z', t) \tag{10c}$$

$$p_f^1(r, \theta, z', t) = p_f^2(r, \theta, z', t) \tag{10d}$$

$$\left(\frac{\partial p_f^1}{\partial z}\right)_{z=z'} = \left(\frac{\partial p_f^2}{\partial z}\right)_{z=z'} \tag{10e}$$

$$\sigma_{zz}^1(r, \theta, z', t) = \sigma_{zz}^2(r, \theta, z', t) \tag{10f}$$

for $r \le 1$,

$$\sigma_{z\theta}^1(r, \theta, z', t) - \sigma_{z\theta}^2(r, \theta, z', t) = \sin\theta \tag{11a}$$

$$\sigma_{zr}^1(r, \theta, z', t) - \sigma_{zr}^2(r, \theta, z', t) = -\cos\theta \tag{11b}$$

and, for $r > 1$,

$$\sigma_{z\theta}^1(r, \theta, z', t) - \sigma_{z\theta}^2(r, \theta, z', t) = 0 \tag{11c}$$

$$\sigma_{zr}^1(r, \theta, z', t) - \sigma_{zr}^2(r, \theta, z', t) = 0. \tag{11d}$$

Representing the prescribed traction in eqns (11) by a single expression of a Laplace-Hankel transform leads to

$$\sigma_{z\theta}^1(r, \theta, z', t) - \sigma_{z\theta}^2(r, \theta, z', t) = \frac{\sin\theta}{2\pi i}\int_0^\infty \int_{\alpha-i\infty}^{\alpha+i\infty} J_0(\xi r) J_1(r) J_1(\xi) \frac{e^{pt}}{p}\, dp\, d\xi \tag{12a}$$

$$\sigma_{zr}^1(r, \theta, z', t) - \sigma_{zr}^2(r, \theta, z', t) = -\frac{\cos\theta}{2\pi i}\int_0^\infty \int_{\alpha-i\infty}^{\alpha+i\infty} J_0(\xi r) J_1(\xi) \frac{e^{pt}}{p} dp\, d\xi. \tag{12b}$$

Substituting eqns (3) and (6), in view of eqns (4) and (7), into eqns (9), (10) and (12) leads to a system of twelve simultaneous equations from which the twelve constants are obtained.

Linearly varying normal force on the surface of the half-space

For the case of a normal force with a linearly varying intensity over a circular area of a radius a on the surface of the half-space as shown in Fig. 2, the problem can be solved in a similar manner as in the previous case, but involves only domain 2, and conditions are the following. For $z = 0$, $t > 0$ and $0 \le r < \infty$,

$$\sigma_{z\theta}^2(r, \theta, 0, t) = 0, \qquad \sigma_{zr}^2(r, \theta, 0, t) = 0 \tag{13a, b}$$

$$p_f^2(r, \theta, 0, t) = 0 \tag{13c}$$

and, for $r \leq 1$,

$$\sigma_{zz}^2(r, \theta, 0, t) = r \cos \theta \tag{14a}$$

but, for $r > 1$,

$$\sigma_{zz}^2(r, \theta, 0, t) = 0. \tag{14b}$$

Representing the prescribed traction in eqns (14) by a single expression of a Laplace–Hankel transform leads to

$$\sigma_{zz}^2(r, \theta, 0, t) = \frac{\cos \theta}{2\pi i} \int_0^\infty \int_{\alpha - i\infty}^{\alpha + i\infty} J_1(\xi r) J_2(\xi) \frac{e^{pt}}{p} dp \, d\xi. \tag{15}$$

Substituting eqns (3) and (6), in view of eqns (4) and (7), into eqns (13) and (15) leads to a system of four simultaneous equations; from which the four nonvanishing constants, A_1^2, B_1^2, E_1^2 and G_1^2, can be obtained.

4. A CYLINDRICAL BAR PARTIALLY EMBEDDED IN THE HALF-SPACE

The problem of bending of a circular cylindrical elastic bar partially embedded in a completely saturated and isotropic elastic half-space is depicted in Fig. 3. In addition to those previously defined, following notations are introduced in this system: L denotes the embedded length of the bar; Q_0 and M_0 denote respectively the lateral force and moment applied as time step functions at the top end of the bar which is flush with the surface of the half-space; and x_1, x_2 and x_3 are cartesian coordinates; thus x_1 is identical to r for $\theta = 0$, and x_3 is identical to z. Also it should be recalled that every quantity of length is nondimensionalized by the bar radius a.

Decomposition of the problem

Following the approximative scheme used by Muki and Sternberg[2] in the elastostatic axial load-transfer, the system in Fig. 3 are decomposed into two systems; an extended half-space B as shown in Fig. 4(a), and a fictitious elastic bar B_* as shown in Fig. 4(b) with a Young's modulus E_* equal to the difference between the Young's moduli of the real bar E_p and the half-space E, i.e.

$$E_* = E_p - E. \tag{16}$$

The extended half-space B, which is characterized by the material constants E, ν and c, is subjected to a distribution bond-force $q(z)$ which is exerted by B_* on B at $x_3 = z$ in a region D in place of the bar. In addition, B is also subjected to end forces $Q_0 - Q_*(0)$ and $Q_*(L)$ and an end moment $M_0 - M_*(0)$ applied at the terminal cross sections as shown in Fig. 4(a). The bond-force $q(z)$ and the end forces $Q_0 - Q_*(0)$ and $Q_*(L)$ are assumed to be uniformly

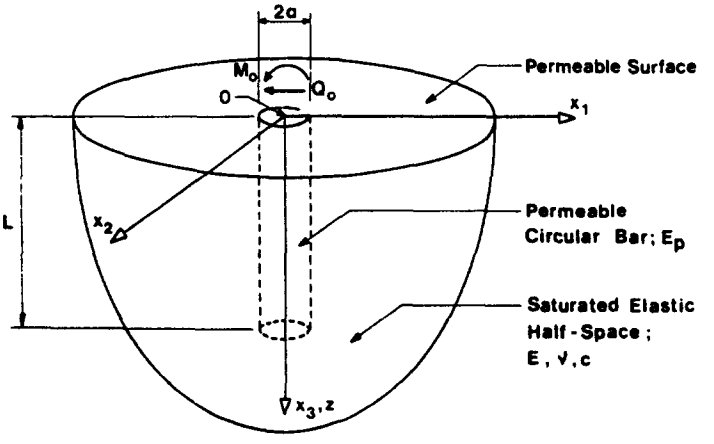

Fig. 3. Geometry of bar and embedding medium.

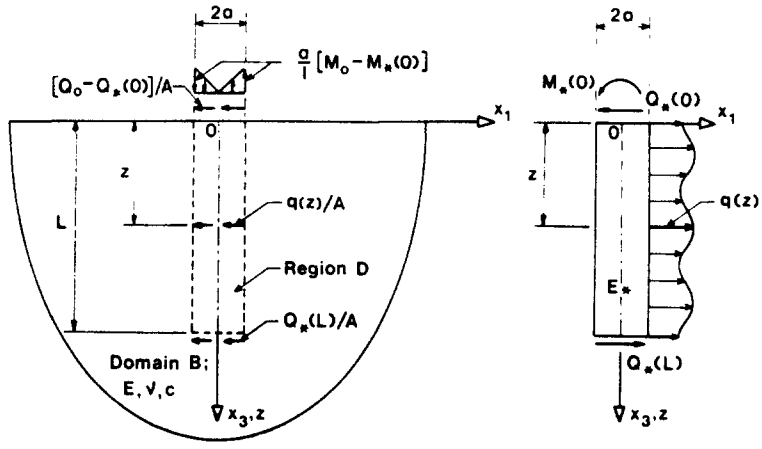

(a) Extended Half-Space B (b) Fictitious Bar B_*

Fig. 4. Composition of the problem.

distributed over their respective cross sections $\bar{\Pi}_z(0<z<L)$, $\bar{\Pi}_0$ and $\bar{\Pi}_L$; while the end moment $M_0-M_*(0)$ is represented at cross section $\bar{\Pi}_0$ by a hydrostatically distributed force, i.e. a normal force as a constant function of x_2 but a linear odd function of x_1.

Conversely, the bond-forces and moment are exerted by the extended half-space B on the fictitious bar B_*, which may be treated as an elementary elastic beam in bending, for which the equations of equilibrium are

$$q(z)=-\frac{dQ_*(z)}{dz} \qquad (0<z<L) \tag{17}$$

$$Q_*(z)=\frac{dM_*(z)}{dz} \qquad (0<z<L) \tag{18}$$

where $Q_*(z)$ and $M_*(z)$ are fictitious shear force and moment, respectively, acting at $x_3=z$.

In this paper, only the case of a permeable bar is treated, yet the results should be accurate enough for practical purposes for the case of an impermeable bar with a large slenderness ratio. The problem will be formulated under the scheme that the displacement of the real bar is equal to that of the fictitious bar B_*, and also equal to the corresponding average over the corresponding cross section of region D in B. The stress resultants in the real bar will be obtained by a superposition of those in B_* with the corresponding integrals over the corresponding cross section of region D in B.

Governing integral equation

To derive the governing integral equation, a bond condition between B_* and B is chosen as that the slope in the plane of loading (x_1x_3-plane) of B_* (Fig. 4b) be equal to the cross sectional average of the corresponding quantity of region D in domain B (Fig. 2a), i.e.,

$$\Psi_*(z)=\frac{1}{A}\int_{\Pi_z}\Psi(\bar{x})dA \qquad (0\le z\le L) \tag{19}$$

where $\bar{x}$ is a position cartesian vector with x_1, x_2 and x_3 as its orthogonal components, A is the nondimensional cross sectional area of the bar and equal to π, $\Psi_*(z)$ is the slope at $x_3=z$ of B_*, and $\Psi(\bar{x})$ is the derivative with respect to z of the displacement in x_1-direction at a point $\bar{x}$ in the domain B.

The slope $\Psi_*(z)$ of B_* can be taken as a superposition of the slope of the fictitious bar assumed to have a zero slope at $x_3=L$, with a rigid body rotation, i.e.

$$\Psi_*(z)=\int_0^L \Psi_b(z,z')q(z')dz'-Q_*(0)\Psi_b(z,0)+\frac{M_*(0)}{E_*I}(L-z)+\Psi_0 \quad (0\le z\le L) \tag{20}$$

where I is the nondimensional moment of inertia of the bar cross section and equal to $\pi/4$, ψ_0 denotes the rigid body rotation, and

$$\Psi_b(z, z') = -\frac{1}{2E_*I}(L-z')^2 \qquad (0 \le z \le z') \tag{21a}$$

$$= -\frac{1}{2E_*I}(L-z)(L-2z'+z) \qquad (z' \le z \le L). \tag{21b}$$

For B, the function $\Psi(\bar{x})$ in eqn (19) can be expressed in the form

$$\Psi(\bar{x}) = \frac{1}{A}[Q_0 - Q_*(0)]\Psi_Q(\bar{x}, 0) + \frac{Q_*(L)}{A}\Psi_Q(\bar{x}, L)$$
$$+\frac{1}{I}[M_0 - M_*(0)]\Psi_M(\bar{x}) + \frac{1}{A}\int_0^L \Psi_Q(\bar{x}, z')q(z')\mathrm{d}z' \tag{22}$$

where $\Psi_Q(\bar{x}, z')$ and $\Psi_m(\bar{x})$ are constituents of the fundamental solutions; $\Psi_Q(\bar{x}, z')$ is the derivative of the displacement in x_1 -direction with respect to z at a point $\bar{x}$ in the half-space due to a uniform shearing force as shown in Fig. 1, while $\Psi_M(\bar{x})$ is the same type of derivative due to a hydrostatically distributed force as shown in Fig. 2.

Substituting eqns (20) and (22) into eqn (19), in view of eqn (17), yields

$$-\int_0^L \Psi_b(z, z')\frac{\mathrm{d}Q_*(z')}{\mathrm{d}z'}\mathrm{d}z' - Q_*(0)\Psi_b(z, 0) + \frac{M_*(0)}{E_*I}(L-z) + \Psi_0$$
$$= \frac{1}{A}[Q_0 - Q_*(0)]\Psi_Q^0(z, 0) + \frac{Q_*(L)}{A}\Psi_Q^0(z, L) + \frac{1}{I}[M_0 - M_*(0)]\Psi_M^0(z)$$
$$-\frac{1}{A}\int_0^L \Psi_Q^0(z, z')\frac{\mathrm{d}Q_*(z')}{\mathrm{d}z'}\mathrm{d}z' \qquad (0 \le z \le L) \tag{23}$$

where $\Psi_Q^0(z, z')$ and $\Psi_M^0(z)$ are influence functions defined as

$$\Psi_Q^0(z, z') = \frac{1}{A}\int_{\Pi_z} \Psi_Q(\bar{x}, z')\mathrm{d}A \qquad (0 \le z, z' \le L, z \ne z') \tag{24a}$$

$$\Psi_M^0(z) = \frac{1}{A}\int_{\Pi_z} \Psi_M(\bar{x})\mathrm{d}A \qquad (0 \le z \le L) \tag{24b}$$

thus can be obtained from the fundamental solutions, and are given in Appendix for final and initial solutions.

It should be noted that the influence function $\Psi_Q^0(z, z')$ is smooth and continuous everywhere except at $z = z'$, where the magnitude of the discontinuity of the shearing stress in x_1-direction is unity. Thus the discontinuity of $\Psi_Q^0(z, z')$ at $z = z'$ is

$$\Psi_Q^0(z, z^+) - \Psi_Q^0(z, z^-) = -\frac{1}{G}. \tag{25}$$

Integrating the integrals in eqns (23) by parts while taking a proper account of the discontinuities at $z = z'$ of eqn (25), and imposing that the curvatures of the fictitious bar B_* and the real bar at $x_3 = 0$ are equal, i.e.

$$M_*(0) = \frac{E_*}{E_p}M_0 \tag{26}$$

yield

$$\frac{Q_*(z)}{GA} - \int_0^L \frac{Q_*(z')}{A}\frac{\partial \Psi_Q^0(z, z')}{\partial z'}\mathrm{d}z' + \int_0^L Q_*(z')\frac{\partial \Psi_b(z, z')}{\partial z'}\mathrm{d}z'$$

$$= \frac{Q_0}{A}\Psi_Q^0(z, 0) + \frac{M_0}{E_p I}[E\Psi_M^0(z) - (L - z)] - \Psi_0 \qquad (0 \le z \le L). \tag{27}$$

Equation (27) which is in the form of a Fredholm integral equation of the second kind may be viewed as the governing integral equation of this problem. Assuming that the function $Q_*(z)$ is a smooth continuous function in the interval $0 \le z \le L$, this governing integral equation is readily amendable to a numerical solution. However, the value of $Q_*(z)$ determined from this equation is a linear combination of the applied loadings Q_0 and M_0, and the unknown rigid body rotation Ψ_0 of B_*. The next necessary step is to determine Ψ_0 by noting that the bending moment in B_* vanishes at $x_3 = L$, and this implies, due to eqns (18) and (26), that

$$\int_0^L Q_*(z)\mathrm{d}z = -\frac{E_*}{E_p}M_0 \tag{28}$$

Substituting the values of $Q_*(z)$ obtained from the governing eqn (27) into eqn (28) yields a simple linear equation for obtaining the value of Ψ_0 in terms of the applied loadings Q_0 and M_0.

At an early stage of this paper, it was found that if the curvature instead of the slope is taken as the bond condition between B_* and B, the analysis would not involve the rigid body rotation Ψ_0, but the kernel in the governing integral equation is highly singular at $z = z'$ and nonintegrable.

Stress resultants and displacements

The real shear force $Q(z)$ is obtained by combining the fictitious shear force $Q_*(z)$ with the area integral of the corresponding shearing stress in region D of B, i.e.

$$Q(z) = Q_*(z) + \int_{\Pi_z} \sigma_{31}(\bar{x})\mathrm{d}A \qquad (0 \le z \le L) \tag{29}$$

where $\sigma_{31}(\bar{x})$ is the shearing stress in x_1-direction at point $\bar{x}$ in domain B. Similarly, the real bending moment $M(z)$ is obtained by combining the fictitious moment $M_*(z)$ with the area integral of the moment about x_2 -axis of the effective normal stress in region D of domain B, i.e. in view of eqns (18) and (26),

$$M(z) = \frac{E_*}{E_p}M_0 + \int_0^z Q_*(z')\mathrm{d}z' + \int_{\Pi_z} [\sigma_{33}(\bar{x}) - p_f(\bar{x})]x_1\,\mathrm{d}A \qquad (0 \le z \le L) \tag{30}$$

where $\sigma_{33}(\bar{x})$ and $p_f(\bar{x})$ are normal stress in x_3 -direction and excess pore pressure, respectively, at point $\bar{x}$ in domain B. The displacement of the real bar in x_1-direction $u_*(z)$ is equal to the average over Π_z of the corresponding displacement in region D of domain B, i.e.

$$u_*(z) = \frac{1}{A}\int_{\Pi_z} u(\bar{x})\mathrm{d}A \qquad (0 \le z \le L) \tag{31}$$

where $u(\bar{x})$ is the displacement at the point $\bar{x}$ in domain B in x_1 -direction. By performing appropriate integrations of the fundamental solutions derived in the previous section (Figs. 1 and 2), eqns (29)–(31) can be put in the forms

$$Q(z) = Q_0\sigma_{31}^0(z, 0) + \frac{AEM_0}{IE_p}\sigma_{31M}^0(z) + \int_0^L Q_*(z')\frac{\partial \sigma_{31Q}^0(z, z')}{\partial z'}\mathrm{d}z' \quad (0 \le z \le L) \tag{32}$$

$$M(z) = Q_0[\sigma_{33Q}^0(z,0) - p_{fQ}^0(z,0)] + M_0\left\{\frac{E_*}{E_p} + \frac{AE}{IE_p}[\sigma_{33M}^0(z) - p_{fM}^0(z)]\right\}$$
$$+ \int_0^L Q_*(z')\frac{\partial}{\partial z'}[\sigma_{33Q}^0(z,z') - p_{fQ}^0(z,z')]\mathrm{d}z'$$
$$+ \int_0^z Q_*(z')\mathrm{d}z' \qquad (0 \le z \le L) \tag{33}$$

$$u_*(z) = \frac{Q_0}{A}u_Q^0(z,0) + \frac{EM_0}{IE_p}u_M^0(z) + \int_0^L \frac{Q_*(z')}{A}\frac{\partial u_Q^0(z,z')}{\partial z'}\mathrm{d}z \quad (0 \le z \le L) \tag{34}$$

where $\sigma_{31Q}^0(z,z')$, $\sigma_{31M}^0(z)$, $\sigma_{33Q}^0(z,z')$, $\sigma_{33M}^0(z)$, $p_{fQ}^0(z,z')$, $p_{fM}^0(z)$, $u_Q^0(z,z')$ and $u_M^0(z)$ are influence functions defined as

$$\sigma_{31Q}^0(z,z') = \frac{1}{A}\int_{\Pi_z} \sigma_{31Q}(\bar{x},z')\mathrm{d}A \tag{35a}$$

$$\sigma_{31M}^0(z) = \frac{1}{A}\int_{\Pi_z} \sigma_{31M}(\bar{x})\mathrm{d}A \tag{35b}$$

$$\sigma_{33Q}^0(z,z') = \frac{1}{A}\int_{\Pi_z} \sigma_{33Q}(\bar{x},z')x_1\,\mathrm{d}A \tag{35c}$$

$$\sigma_{33M}^0(z) = \frac{1}{A}\int_{\Pi_z} \sigma_{33M}(\bar{x})x_1\,\mathrm{d}A \tag{35d}$$

$$p_{fQ}^0(z,z') = \frac{1}{A}\int_{\Pi_z} p_{fQ}(\bar{x},z')x_1\,\mathrm{d}A \tag{35e}$$

$$p_{fM}^0(z) = \frac{1}{A}\int_{\Pi_z} p_{fM}(\bar{x})x_1\,\mathrm{d}A \tag{35f}$$

$$u_Q^0(z,z') = \frac{1}{A}\int_{\Pi_z} u_Q(\bar{x},z')\mathrm{d}A \tag{35g}$$

$$u_M^0(z) = \frac{1}{A}\int_{\Pi_z} u_M(\bar{x})\mathrm{d}A. \tag{35h}$$

In eqns (32)–(35), subscript Q denotes the fundamental solution corresponding to Fig. 1, and subscript M denotes the fundamental solution corresponding to Fig. 2. In addition, the integrals in eqns (35) are constituents of the fundamental solutions. The influence functions defined by equations (24) and (35) are given in detail in Appendix for final and initial solutions.

Another quantity of interest in this problem is the slope of the real bar, which may be taken as identical to $\Psi_*(z)$ in eqn (20). Substituting eqns (17) and (26) into eqn (20) and integrating by parts yield

$$\Psi_*(z) = \int_0^L Q_*(z')\frac{\partial \Psi_b(z,z')}{\partial z'}\mathrm{d}z' + \frac{M_0}{E_pI}(L-z) + \Psi_0 \qquad (0 \le z \le L). \tag{36}$$

Final solution

As time t approaches infinity, the excess pore pressure tends to zero and the solution of this problem becomes identical to the ideal elastostatic solution. The final fundamental solutions, which can be either solved directly according to the theory of ideal elasticity or specialized from the transient problem presented in Section 3 by putting p to zero, are given in the Appendix.

For this case, the kernel $(\partial \Psi_Q^0(z,z')/\partial z')$ involved in the governing integral equation, eqn (27), can be shown to have an integrable logarithmic singularity at $z = z'$. Muki and Sternberg[2] solved an integral equation of this type by a numerical scheme in which the kernel is separated into a singular and a continuous portions. The range of integration was partitioned uniformly and the unknown function Q_* was assumed to be a continuous function and linear between two consecutive mesh-points of the interval. The contribution to the improper integral from the

singular portion of the kernel was evaluated in closed elementary form in terms of the values of Q_* at the mesh-points, and the contribution to the integral from the continuous portion of the kernel was computed by means of trapezoidal rule.

It is found that such a numerical solution was not very efficient for solving this type of integral equation. Following the solution scheme used sucessfully by Hopkins and Hamming[13] and Lee and Rogers[14] in the solution of Volterra integral equations: the range of integration are divided into n equal partitions and $Q_*(z)$ in each partition is replaced by the arithematic mean of its two nodal values, thus eqn (27) becomes

$$\frac{Q_*(z_i)}{GA} - \sum_{j=1}^{n} \frac{1}{2}[Q_*(z_j) + Q_*(z_{j+1})]\{[\Psi_Q{}^0(z_i, z_{j+1}) - \Psi_Q{}^0(z_i, z_j)]/A + [\Psi_b(z_i, z_{j+1}) - \Psi_b(z_i, z_j)]\} = \frac{Q_0}{A}\Psi_Q{}^0(z_i, 0) + \frac{M_0}{E_p I}[E\Psi_M{}^0(z_i) - (L - z_i)] - \Psi_0. \tag{37}$$

Equation (37) is a system of $n+1$ simultaneous equations, in which the unknowns are values of Q_* at z_i for $i = 1$ to $n+1$ with $z_1 = 0$ and $z_{n+1} = L$. Substituting the values of Q_* obtained by solving eqn (37) into eqn (28) which can be written in the form

$$\sum_{j=1}^{n} \frac{L}{2n}[Q_*(z_j) + Q_*(z_{j+1})] = -\frac{E_*}{E_p} M_0 \tag{38}$$

yields the value of the rigid body rotation Ψ_0. Once Ψ_0 is found, the solution of Q_* is complete in terms of Q_0 and M_0 only. Subsequently, the determination of the real shear force, moment, displacement and slope of the real bar as defined by eqns (32)–(34) and (36) are straight-forward by using the same technique of numerical integration.

Numerical results for a separate application of Q_0 and M_0 are obtained; and the reciprocal condition, i.e. the rotation due to $Q_0 = 1$ and the displacement due to $M_0 = 1$ at $z = 0$ should be equal, is used as an indicator of the accuracy of the results. As should be expected, the accuracy of the results improves with the increase of the number of partitions n, and a more flexible (high EL^4/E_p) bar requires a bigger n than a stiffer (low EL^4/E_p) one. It is suggested herein to use $n = 50$ for $L = 5$ and 10, $n = 100$ for $L = 20$ and 50, and $n = 150$ for $L = 150$ and 200.

Initial solution

The technique of solving the initial solution is similar to that used in the final solution. The influence functions involved can be specialized from the transient solution by simply letting p approach infinity after all limits of z variable are reached. The resulting influence functions and the additional influence pore pressure are given in detail in the Appendix

6. PARAMETRIC STUDY AND DISCUSSION OF RESULTS

Parametric study

The parameters in this paper are the length-radius ratio L of the bar, the modulus ratio between the bar and the medium E_p/E, the Poisson's ratio ν of the medium. The final and initial results of the bar shear force, moment and displacement are given for different parameters within the range of practical values as shown in Figs. 5–16.

Discussion of results

Figures 5 and 6 show the typical results of the final and initial solutions plotted along the length of the bar, while Figs. 7–16 show the effects of ν, L and E_p/E. From these figures, it can be seen that the initial quantities are significantly smaller than the final quantities in displacement and moment, but less so in shear force. However, for bars with high values of E_p/E and large values of L, both solutions are very close to each other in all respects. In addition, it should be noted that the effects of L and E_p/E on the final and initial solutions are significant, but the effect of Poisson's ratio ν is small in most cases, except on the displacement due to the lateral force Q_0 especially for bars with small values of E_p/E.

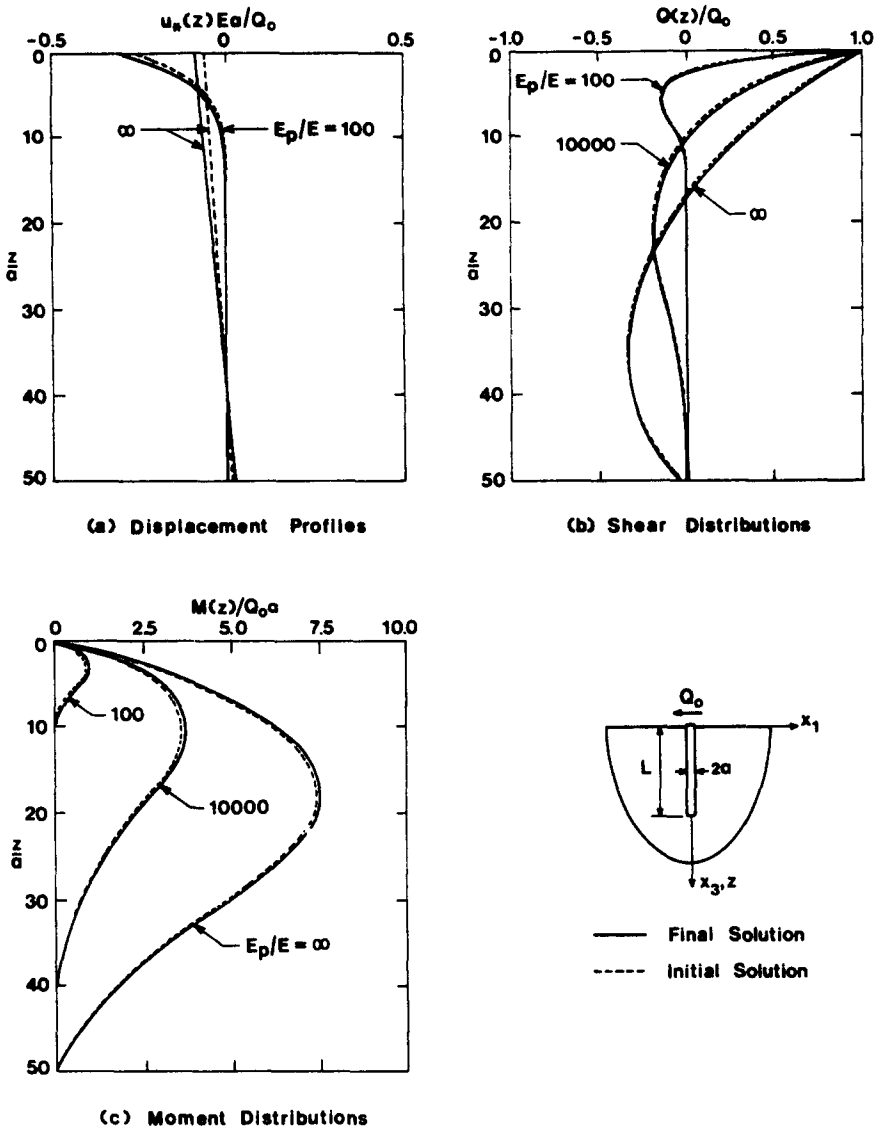

Fig. 5. Solution for $L = 50$, $\nu = 0.25$; due to Q_0 only.

As an illustrative example and a comparison with other existing results; consider the case of the hexagonal hollow steel pile, with a gross cross sectional area = 888 cm^2 and a flexural rigidity = 1600 tons-m^2, investigated by Kerisel and Adam[15]. The pile, which is embedded by 4.65 m in a clay medium, is laterally loaded at the height 1.15 m above the medium surface. In order to apply the proposed solution, the tested pile is represented by a circular cylindrical bar of the same flexural rigidity and the same gross cross section area; resulting in $E_p = 2.55 \times 10^6$ tons/m^2 and $a = 16.82$ cm. The measured and theoretical displacements at the ground surface is equated to obtain the Young's modulus of soil $E = 1110$ tons/m^2, and the Poisson's ratio is taken as 0.50. The results obtained by the proposed final solution is shown in Fig. 17 together with the measured value[15] and the predicted solution by Poulos[5] for a load of 6 tons, which is well below the ultimate capacity of the system. The profiles by the proposed solution are shown to be in close aggrement with the ones measured.

7. CONCLUSIONS

A rational study on the quasi-static bending of a circular cylindrical elastic bar partially embedded in a saturated elastic half-space is presented here. The governing integral equation, which is formulated under the approximation that the slope of the fictitious bar is equal to the corresponding average over a corresponding circular area in the extended half-space, involves

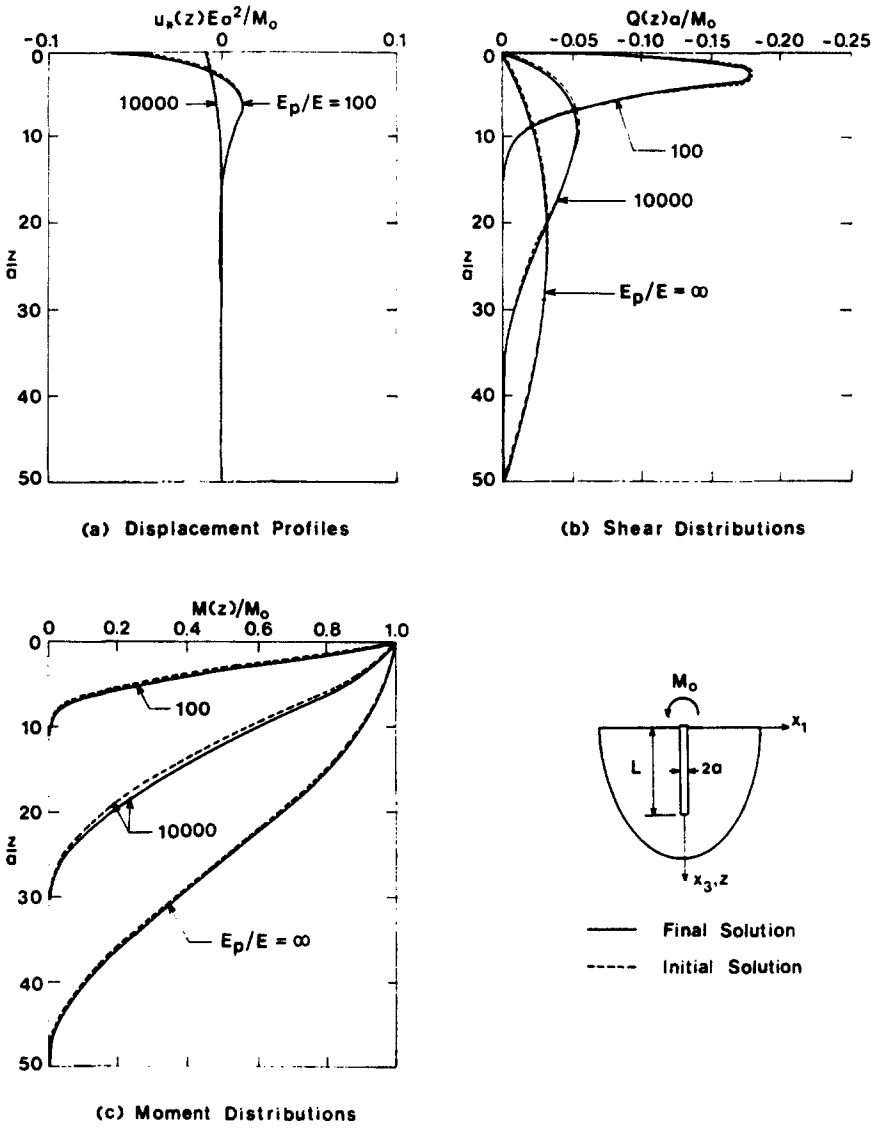

Fig. 6. Solution for $L = 50$, $\nu = 0.25$; due to M_0 only.

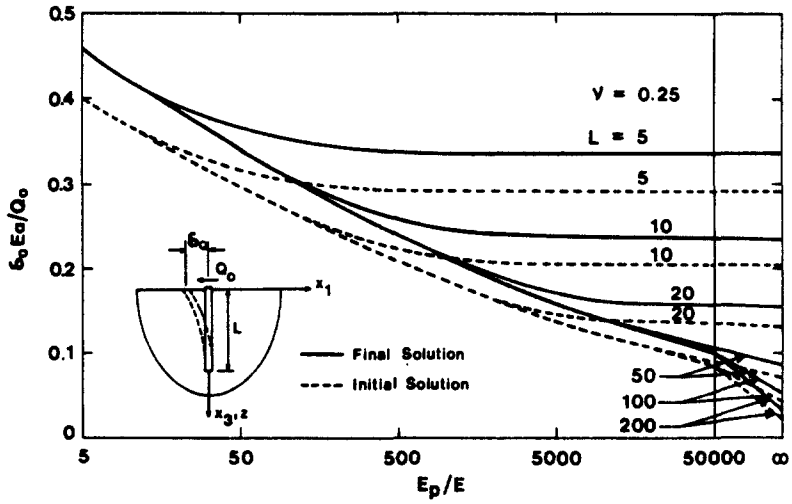

Fig. 7. Effects of L on bar tip displacement due to Q_0.

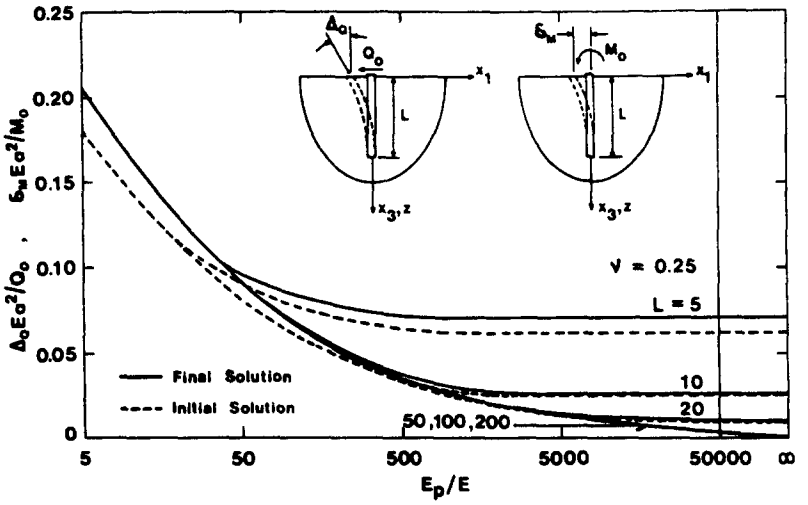

Fig. 8. Effects of L on bar tip rotation due to Q_0 and on bar tip displacement due to M_0.

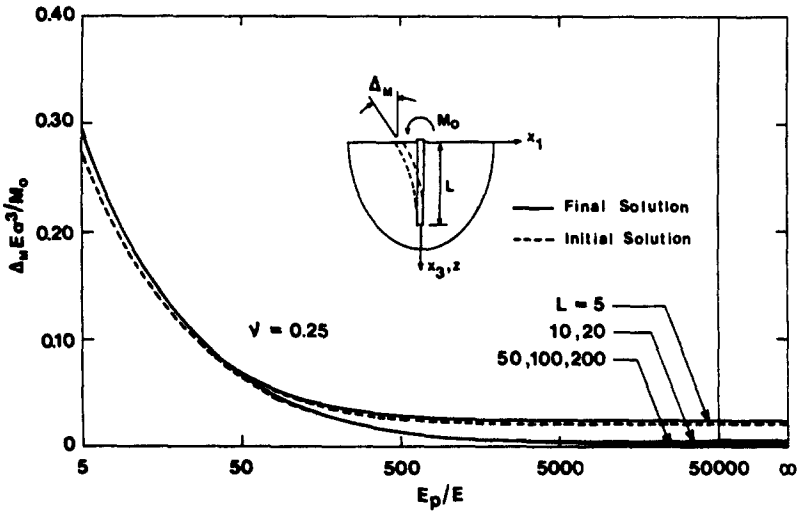

Fig. 9. Effect of L on bar tip rotation due to M_0.

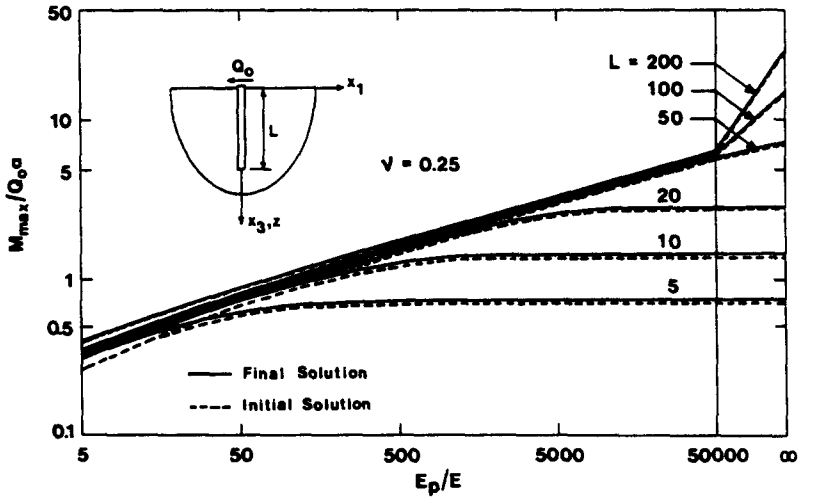

Fig. 10. Effect of L on maximum moment of bar due to Q_0.

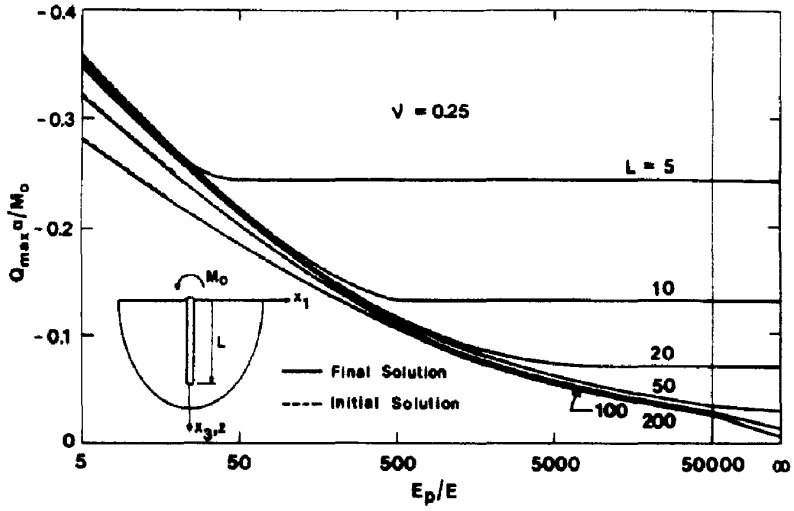

Fig. 11. Effect of L on maximum shear force of bar due to M_0.

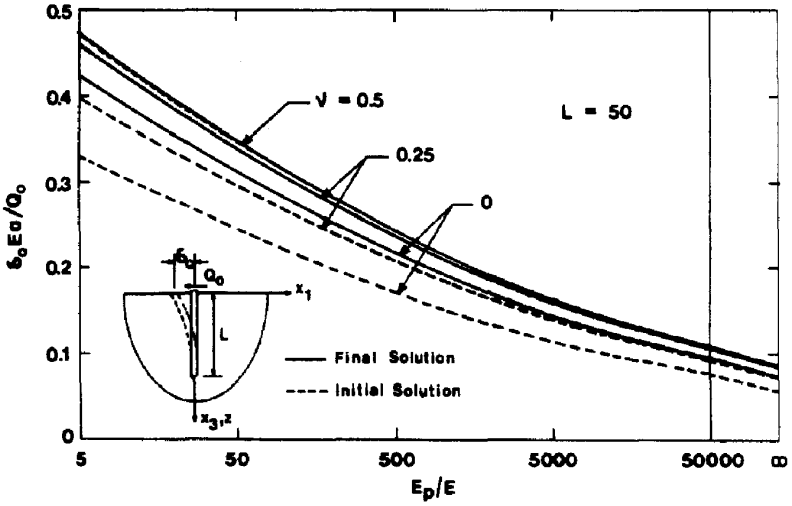

Fig. 12. Effect of Poisson's ratio ν on bar tip displacement due to Q_0.

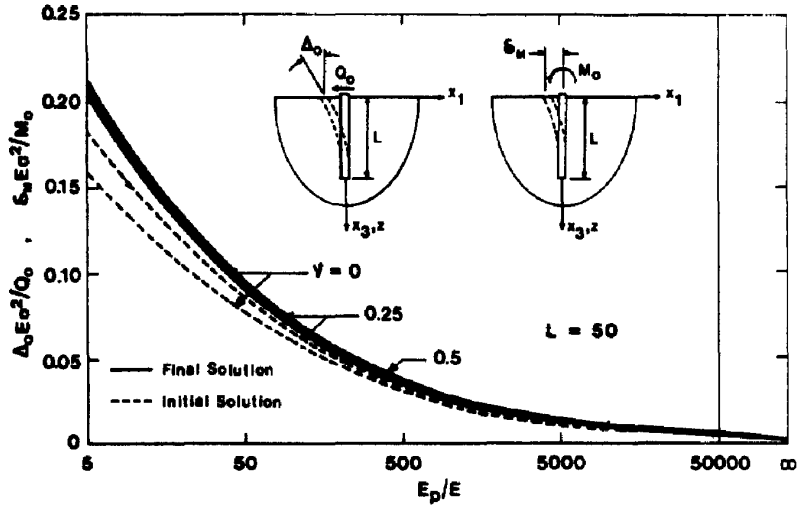

Fig. 13. Effect of Poisson's ratio ν on bar tip rotation due to Q_0 and on bar tip displacement due to M_0.

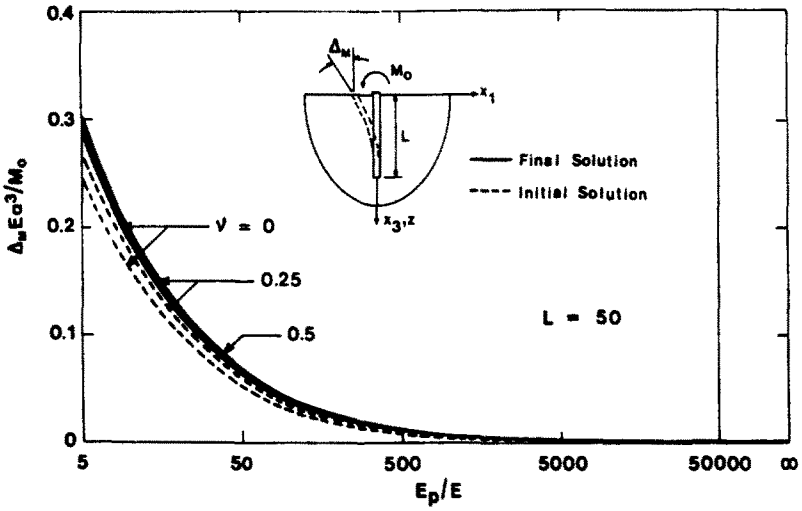

Fig. 14. Effect of Poisson's ratio ν on bar tip rotation due to M_0.

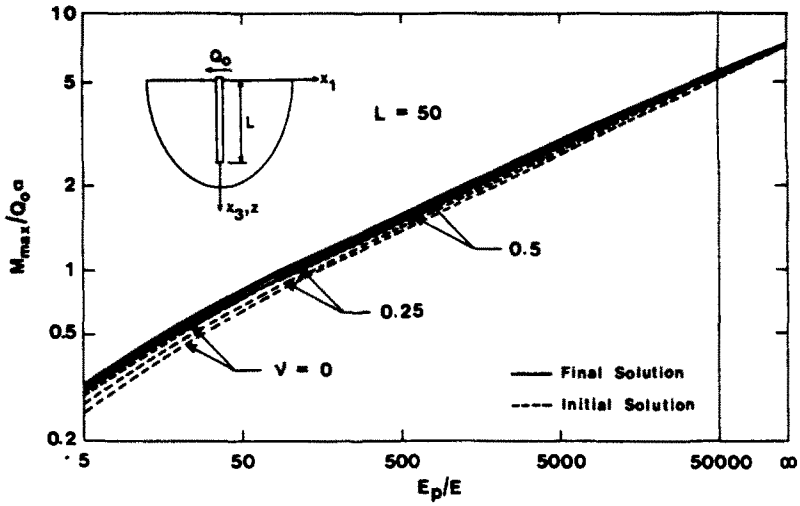

Fig. 15. Effect of Poisson's ratio ν on maximum moment of bar due to Q_0.

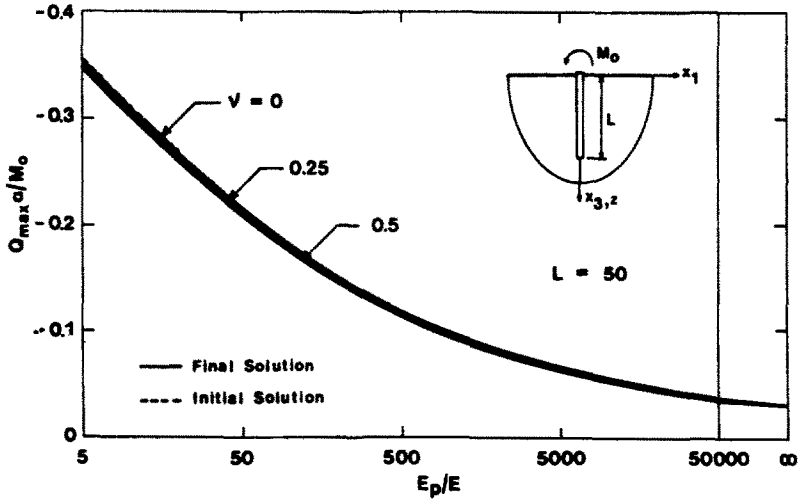

Fig. 16. Effect of Poisson's ratio ν on maximum shear force of bar due to M_0.

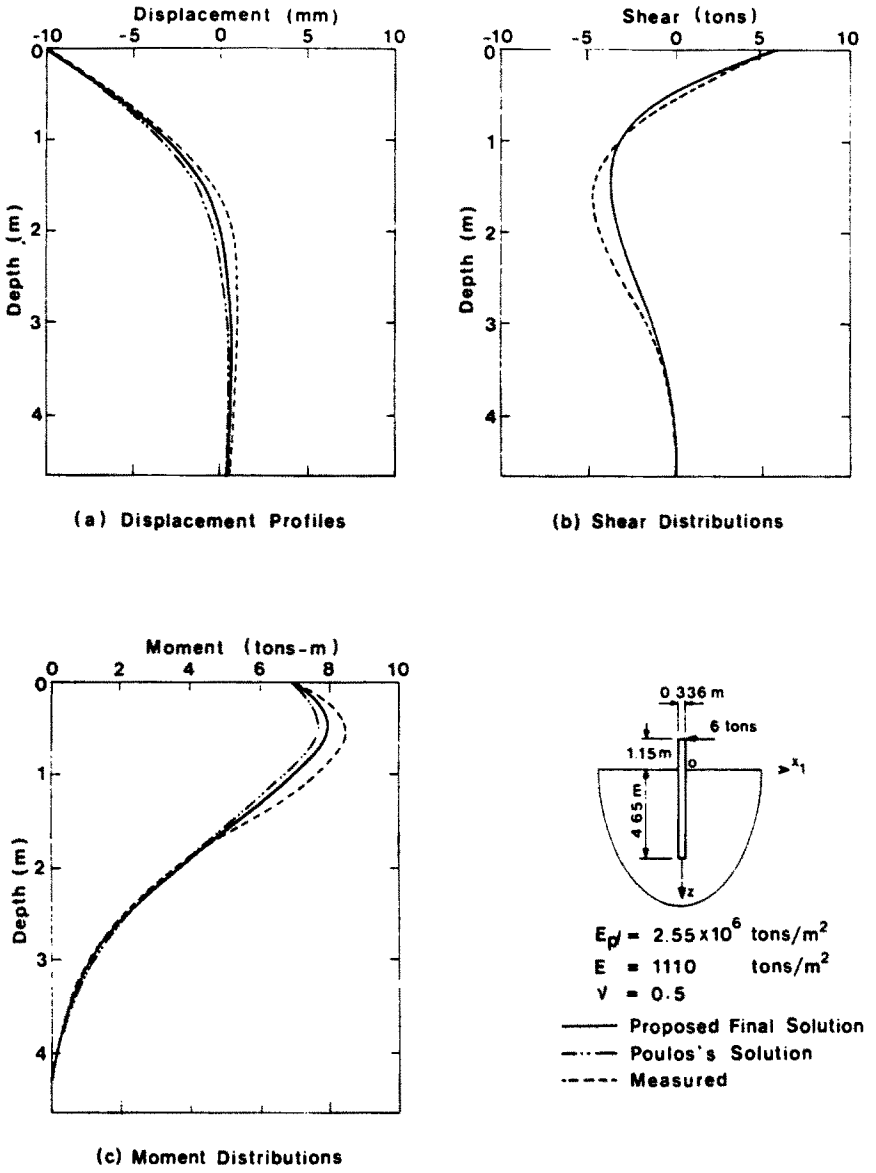

Fig. 17. Comparison of proposed final solution with that by Poulos[5] and a field measurement by Kerisel and Adam[15].

an additional unknown rigid body rotation of the fictitious bar, which are determined subsequently by the condition of zero bending moment at the lower end of the fictitious bar. It is found that if the curvature instead of the slope is taken as the bond condition between the fictitious bar and the half-space; the analysis, though not involving such unknown rigid body rotation, is not successful, since the kernel in the governing integral equation becomes nonintegrable.

Only results of the final and initial solutions are attempted, since they should be sufficient for most practical cases. If needed, the numerical results of the transient solution not given here, may be obtained by a modified Ritz's method as described by Niumpradit[3] for the case of axisymmetric loading.

Also it should be mentioned: The proposed approach is valid for the condition of small displacements. The embedded bar as well as the embedding medium are assumed to remain elastic. The medium are considered to be homogeneous, isotropic and completely saturated. The bar, if not permeable, must be slender enough, so that the condition of permeability can be assumed. A direct treatment for the case of an impermeable bar is obviously very complicated.

Acknowledgements—The present paper is based in part on the dissertation by the first author[16], which was submitted in partial fulfillment of the requirements for the degree of Doctor of Engineering at the Asian Institute of Technology. The authors are indebted to the Dissertation External Examiner, Professor John Dundurs of Northwestern Universtiy, for his review comments and suggested corrections.

REFERENCES

1. R. Muki and E. Sternberg, On the diffusion of an axial load from an infinite cylindrical bar embedded in an elastic medium. *Int. J. Solids Struct.* **5**, 587 (1969).
2. R. Muki and R. Sternberg, Elastostatic load-transfer to a half-space from a partially embedded axially loaded rod. *Int. J. Solids Struct.* **6**, 69 (1970).
3. B. Niumpradit, Quasi-static axial load-transfer to a saturated porous elastic half-space from an embedded elastic rod. *D. Engng. Dissertation*, Asian Institute of Technology, Bangkok, Thailand (1978).
4. W. R. Spillers and R. D. Stoll, Lateral response of piles. *J. Soil Mech. and Found. ASCE.* **90**, 1 (1964).
5. H. G. Poulos, Behavior of laterally loaded piles; I-Single piles. *J. Soil Mech. and Found. ASCE.* **97**, 711 (1971).
6. M. A. Biot, General theory of three-dimensional consolidation. *J. Appl. Phys.* **12**, 155 (1941).
7. M. A. Biot, Theory of deformation of a porous viscoelastic anisotropic solid. *J. Appl. Phys.* **27**, 459 (1956).
8. M. A. Biot, Mechanics of deformation and acoustic propagation in porous media. *J. Appl. Phys.* **33**, 1482 (1962).
9. R. L. Schiffman and A. A. Fungaroli, Consolidation due to tangential loads. *Proc. 6th Int. Conf. Soil Mech. and Found. Engng.*, 188 (1965).
10. R. Muki, Asymmetric problems of the theory of elasticity for a semi-infinite solid and a thick plate. *Progress in Solid Mechanics* 1, (Edited by I. N. Sneddon and R. Hill) Amsterdam North Holland, Interscience, New York, 399 (1960).
11. R. A. Schapery, Approximate methods of transform inversion for visco-elastic stress analysis. *Proc. 4th U.S. National Cong. Appl. Mech.*, 1075 (1962).
12. G. Eason, B. Noble and I. N. Sneddon, On certain integrals of Lipschitz-Hankel type involving products of Bessel functions. *Phil. Trans. R. Soc. London* **A247**, 529 (1955).
13. I. L. Hopkins and R. W. Hamming, On creep and relaxation. *J. Appl. Phys.* **28**, 906 (1957).
14. E. H. Lee and T. G. Rogers, Solution of viscoelastic stress analysis problems using measured creep and relaxation functions. *J. Appl. Mech. ASME* **30**, 127 (1963).
15. J. Kerisel and M. Adam, Calcul des forces horizontales applicables aux fondations peofondes dans les argiles et limons. *Annales de l'Institute Technique du Batiment et des Travaux Publics* **239**, 1653 (1967).
16. V. Apirathvorakij, Quasi-static bending of cylindrical elastic bar partially embedded in a saturated elastic half-space. *D. Engng. Dissertation*, Asian Institute of Technology, Bangkok, Thailand (1979).
17. M. Abramowitz and I. A. Stegun, *Handbook of Mathematical Functions*, p. 591. Dover Pub. Inc., New York (1972).

APPENDIX-INFLUENCE FUNCTIONS

Influence functions for final solution

For the case of the final (infinite time) solution, the excess pore pressure vanishes, and the remained influence functions defined in eqns (24) and (35) are given for $0 \le z, z' \le L$ and $z \ne z'$ as follows:

$$\Psi_Q^0(z,z') = \frac{1}{8(1-\nu)G}\{8(1-\nu)\bar{h}(z-z')R_1(|z-z'|) - (z-z')R_2(|z-z'|) + 4(1-\nu)(3-2\nu)R_1(z+z') - [(3-4\nu)(z+z')+2z']R_2(z+z') + 2zz'R_3(z+z') \quad (39a)$$

$$\Psi_M^0(z) = \frac{1}{2G}[2(1-\nu)S_1(z) - zS_2(z)] \quad (39b)$$

$$\sigma_{31Q}^0(z,z') = \frac{1}{4(1-\nu)}\{4(1-\nu)\bar{h}(z-z')R_1(|z-z'|) - (z-z')R_2(|z-z'|) + 4(1-\nu)R_1(z+z') - [(3-4\nu)z+z']R_2(z+z') + 2zz'R_3(z+z')\} \quad (39c)$$

$$\sigma_{31M}^0(z) = -zS_2(z) \quad (39d)$$

$$\sigma_{33Q}^0(z,z') = \frac{1}{4(1-\nu)}\{-(1-2\nu)S_1(|z-z'|) + (z-z')\bar{h}(z-z')S_2(|z-z'|) + (1-2\nu)S_1(z+z') + [(3-4\nu)z-z']S_2(z+z') - 2zz'S_3(z+z') \quad (39e)$$

$$\sigma_{33M}^0(z) = N_1(z) + zN_2(z) \quad (39f)$$

$$u_Q^0(z,z') = \frac{1}{8(1-\nu)G}\{-(7-8\nu)R_0(|z-z'|) + (z-z')\bar{h}(z-z')R_1(|z-z'|) - (9-16\nu+8\nu^2)R_0(z+z') + (3-4\nu)(z+z')R_1(z+z') - 2zz'R_2(z+z')\} \quad (39g)$$

$$u_M^0(z) = \frac{1}{2G}[-(1-2\nu)S_0(z) + zS_1(z)] \quad (39h)$$

where

$$\bar{h}(z-z') = -1, \quad z < z'$$
$$= 1, \quad z > z' \quad (40)$$

and R_n, S_n and N_n are integrals of Lipschitz-Hankel type involving products of Bessel functions, i.e.

$$R_n(y) = \int_0^\infty \xi^{n-2} e^{-y\xi} J_1^2(\xi) d\xi \qquad (y > 0, n = 0, 1, 2, 3) \tag{41a}$$

$$S_n(y) = \int_0^\infty \xi^{n-2} e^{-y\xi} J_1(\xi) J_2(\xi) d\xi \qquad (y > 0, n = 0, 1, 2, 3) \tag{41b}$$

$$N_n(y) = \int_0^\infty \xi^{n-2} e^{-y\xi} J_2^2(\xi) d\xi \qquad (y > 0, n = 1, 2). \tag{41c}$$

Due to Eason, Noble and Sneddon[12], these integrals can be put in terms of complete elliptic integrals of first and second kinds, of which numerical values are obtained by means of infinite series[17].

Influence functions for initial solution

For the case of the initial ($t = 0^+$) solution, the influence functions defined in eqns (24) and (35) are specialized from the transient solution by letting p approach infinity after all limits of the z variable are approached. The influence functions in this case can be shown to take the same forms as for the final solution of the incompressible solid, i.e. $\nu = 0.5$. In addition, the influence functions of the excess pore pressure, for $0 \le z, z' \le L$ and $z \ne z'$, are

$$p_{fQ}(z, z') = \frac{1}{2}[S_1(|z - z'|) + S_1(z + z') - 2z' S_2(z + z')] \tag{42a}$$

$$p_{fM}(z) = N_1(z). \tag{42b}$$